29. J. Domen, S. H. Cheshier, I. L. Weissman, *J. Exp. Med.* **191**, 253 (2000).
30. G. G. McGill *et al.*, *Cell* **109**, 707 (2002).
31. E. E. Medrano *et al.*, *Mol. Biol. Cell* **5**, 497 (1994).
32. We thank V. Igras and C. Quigley for technical assistance; L. Lamoreux for supplying *Mitf*^{vit} mice; A. Miller, C. Hershey, and Y. Choi for critical reading of the manuscript; members of the Fisher laboratory for helpful discussions; and D. Rowitch for sharing microscopes. E.K.N. wishes to thank Y. Miyachi for continuous encouragement and support. E.K.N. was supported by the Shiseido Award in 2002 and the Charles A. King Trust, Fleet National Bank, a Bank of America Company, co-trustee (Boston, MA). Supported by grant no. AR43369 from NIH to D.E.F. D.E.F. is the Nirenberg Fellow in pediatric oncology at Dana-Farber Cancer Institute.

Supporting Online Material
www.sciencemag.org/cgi/content/full/1099593/DC1
Materials and Methods
Figs. S1 to S7

26 April 2004; accepted 8 December 2004
Published online 23 December 2004;
10.1126/science.1099593
Include this information when citing this paper.

Dynamic Complex Formation During the Yeast Cell Cycle

Ulrik de Lichtenberg,[1]* Lars Juhl Jensen,[2]* Søren Brunak,[1] Peer Bork[2,3]†

To analyze the dynamics of protein complexes during the yeast cell cycle, we integrated data on protein interactions and gene expression. The resulting time-dependent interaction network places both periodically and constitutively expressed proteins in a temporal cell cycle context, thereby revealing previously unknown components and modules. We discovered that most complexes consist of both periodically and constitutively expressed subunits, which suggests that the former control complex activity by a mechanism of just-in-time assembly. Consistent with this, we show that additional regulation through targeted degradation and phosphorylation by Cdc28p (Cdk1) specifically affects the periodically expressed proteins.

Most research on biological networks has been focused on static topological properties (*1*), describing networks as collections of nodes and edges rather than as dynamic structural entities. Here we focus on the temporal aspects of networks, which allows us to study the dynamics of protein complex assembly during the *Saccharomyces cerevisiae* cell cycle.

Our integrative approach combines protein-protein interactions with information on the timing of the transcription of specific genes during the cell cycle, obtained from DNA microarray time series (*2*, *3*). From the latter, we derived a quality-controlled set of 600 periodically expressed genes, each assigned to the point in the cell cycle where its expression peaks (*4*). We then constructed a physical interaction network for the corresponding proteins from yeast two-hybrid screens (*5*, *6*), complex pull-downs (*7*, *8*), and curated complexes from the Munich Information Center for Protein Sequences (MIPS) database (*9*). To reduce the error rate of 30 to 50% expected in most current large-scale interaction screens (*10*, *11*), all physical interaction data were combined, a topology-based confidence score was assigned to each individual interaction [as in the STRING database (*12*)], and only high-confidence interactions were selected (*13*). These were further filtered with information on subcellular localization (*14*) to exclude interactions between proteins annotated to incompatible compartments (*13*); no curated MIPS interactions were lost because of this filtering. The topology-based scoring scheme, filtering, and extraction criteria reduced the error rate for interactions by an order of magnitude to only 3 to 5% (*13*).

In the extracted network (Fig. 1), we included, in addition to the periodically expressed ("dynamic") proteins, constitutively expressed ("static") proteins that preferentially interact with dynamic ones (*13*). The resulting network consists of 300 proteins (Fig. 1, inside circle), including 184 dynamic proteins (colored according to their time of peak expression) and 116 static proteins (depicted in white). For 412 of the 600 dynamic proteins identified in the microarray analysis, no physical interactions of sufficient reliability could be found (Fig. 1, outside circle). Some may be missed subunits of stable complexes already in the network; the majority, however, probably participate in transient interactions, which are often not detected by current interaction assays (*15*).

Although our procedure for extracting interactions might miss some cellular processes that are dominated by transient interactions, most of the stable complexes should have been captured at least partially. Tandem affinity purifications alone should identify at least half of the subunits for 87% of the known yeast complexes (*7*). Compared with the known cell cycle complexes and functional modules (*9*), we found that all but two of them were identified by our approach (better than random at $P < 10^{-30}$). The only exceptions were the anaphase-promoting complex (APC), which can only be detected with a less stringent interaction cutoff, and the Skp1p/Cullin/F-box protein complex (SCF), which appears to be the only cell cycle–related protein complex without a periodically expressed subunit. For completeness, these two complexes were added to the network. Our extraction procedure produces comparable results even if the curated MIPS complexes are excluded entirely from the analysis or if the specific extraction criteria are changed, showing that the method is robust and has much higher coverage than methods of comparable accuracy (*13*).

The derived cell cycle network (Fig. 1, inside circle) contains 29 heavily intraconnected modules; that is, complexes or groups of complex variants that exist at different time points during the yeast cell cycle. In addition to rediscovering many known cell cycle modules, our approach enables us to place more than 30 poorly characterized proteins in the cell cycle network and to predict new unexpected cell cycle contexts for other proteins (*13*). The network contains 31 isolated binary complexes, many of which involve proteins of unknown function, such as Yml119p and Yll032p, which interact and are both putative Cdc28p substrates (*16*) expressed close in time in G_2 phase (*13*).

As an example of the value of combining temporal data with protein-protein interactions, the network reveals a binary complex consisting of the uncharacterized proteins Ymr295p and Ydr348p. Because only Ydr295p is dynamic, the static protein Ydr348p can only be identified as a cell cycle–relevant protein and placed temporally through the integration of the two complementary data types. Indeed, Ydr348p is a putative Cdc28p target (*16*), and the interaction is further supported by the observation that both proteins localize to the bud neck (*14*). Virtually all complexes contain both dynamic and static subunits (Fig. 1), the latter accounting for about half of the direct interaction partners of periodically regulated proteins through all phases of the cell cycle (Fig. 2). Transcriptional regulation thus influences almost all cell cycle complexes and thereby, indirectly, their static subunits. This implies that many cell cycle proteins cannot be identified through the analysis of any sin-

[1]Center for Biological Sequence Analysis, Technical University of Denmark, DK-2800 Lyngby, Denmark. [2]European Molecular Biology Laboratory, D-69117 Heidelberg, Germany. [3]Max-Delbrück-Centre for Molecular Medicine, D-13092 Berlin, Germany.

*These authors contributed equally to this work.
†To whom correspondence should be addressed. E-mail: bork@embl.de

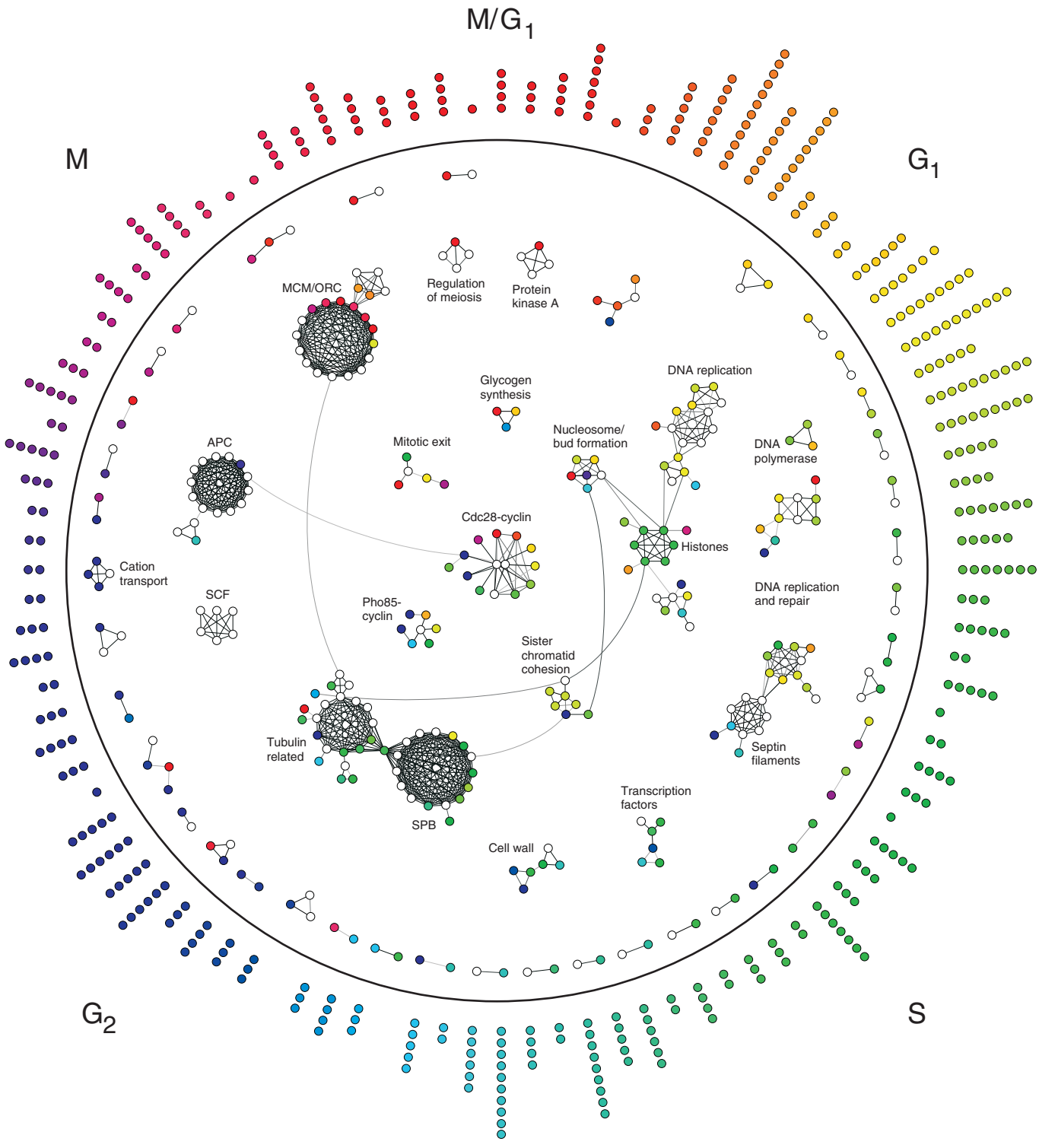

Fig. 1. Temporal protein interaction network of the yeast mitotic cell cycle. Cell cycle proteins that are part of complexes or other physical interactions are shown within the circle. For the dynamic proteins, the time of peak expression is shown by the node color; static proteins are represented by white nodes. Outside the circle, the dynamic proteins without interactions are both positioned and colored according to their peak time and thus also serve as a legend for the color scheme in the network. More detailed versions of this figure (including all protein names) and the underlying data are available online at www.cbs.dtu.dk/cellcycle.

gle type of experimental data but only through integrative analysis of several data types.

In addition to suggesting functions for individual proteins, the network (Fig. 1) indicates the existence of entire previously unknown modules. Most notably, the network reveals a module that includes two poorly characterized proteins (Nis1p and Yol070p) and links processes related to the nucleosomes with mitotic events in the bud (Fig. 3A) (*13*).

Transcription of cell cycle–regulated genes is generally thought to be turned on when or just before their protein products are needed: often referred to as just-in-time synthesis. Contrary to the cell cycle in bacteria (*17*), how-

ever, just-in-time synthesis of entire complexes is rarely observed in the network. The only large complex to be synthesized in its entirety just in time is the nucleosome, all subunits of which are expressed in S phase to produce nucleosomes during DNA replication.

Instead, the general design principle appears to be that only some subunits of each complex are transcriptionally regulated in order to control the timing of final assembly. Several examples of this just-in-time assembly (rather than just-in-time synthesis) are suggested by the network, including the prereplication complex (Fig. 3B), complexes involved in DNA replication and repair, the spindle pole body, proteins related to the cytoskeleton, and numerous smaller complexes or modules (*13*). We find that the transcriptome time mappings visualized in Fig. 1 are in close agreement with previous studies on the dynamic formation of individual protein complexes, suggesting that the timing of transcription of dynamic proteins is indicative of the timing of assembly and action of the complexes and modules (Fig. 3) (*13*). Just-in-time assembly would have an advantage over just-in-time synthesis of entire complexes in that only a few components need to be tightly regulated in order to control the timing of final complex assembly. This would explain the recent observation that the periodic transcription of specific cell cycle genes is poorly conserved through evolution (*18*). For the prereplication complex, exactly this variation between organisms has been shown, although the subunits and the order in which they assemble are conserved (*19*).

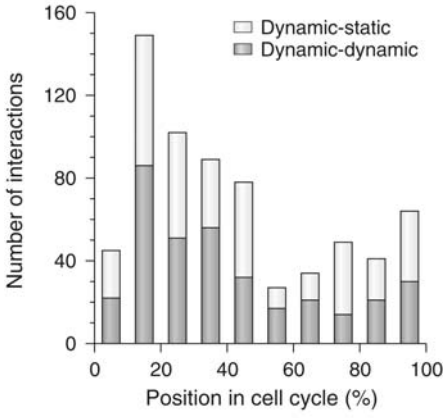

Fig. 2. Interactions during the cell cycle. The number of interactions of dynamic proteins with other dynamic proteins (dynamic-dynamic) and with static proteins (dynamic-static) is shown as a function of cell cycle progression. Zero time corresponds to the time of cell division. The large number of interactions during G_1 phase reflects a general overrepresentation of genes expressed in this part of the cell cycle (Fig. 1).

Dynamic complex assembly also functions as a mechanism for temporal regulation of substrate specificity, best exemplified by the association of the cyclin-dependent kinase Cdc28p with its various transcriptionally regulated cyclins and inhibitors (Fig. 3C). Our approach accurately reproduces this key regulatory system and its temporal dynamics, correctly placing each of the Cdc28p interactions' partners at their time of function and capturing even very transient interactions such as phosphorylation and ubiquitination (Fig. 3C). Transient interactions are also captured between cyclins of the Pho85p system and two M-phase–specific proteins, Swi5p and Mmr1p. Swi5p has already been identified as a Pho85p-Pcl2p substrate (*20*); from the network context, we propose that the uncharacterized phosphoprotein Mmr1p is a target of the Pho85p-Pcl7p kinase (*13*). The cell cycle role of Mmr1p is supported by binding of the transcription factors Fkh2p, Mcm1, and Ndd1p, which cooperatively activate transcription at the G_2/M transition, exactly when the expression of Mmr1p peaks (*21*, *22*).

Furthermore, we used the network model to determine whether the transcriptionally regulated subunits are also regulated by phosphorylation. The 332 putative Cdc28p targets identified in a recent screen (*16*) are indeed much more frequent among the dynamic than among the static proteins in the network [significant at $P < 10^{-4}$ (*13*)]. In the cell cycle network (Fig. 1), 27% of the periodically transcribed proteins are putative Cdc28p targets, in comparison to only 8% of the static proteins and 6% of all yeast proteins. This link between transcriptional and posttranslational control probably reflects multiple roles: It allows the control of complex assembly by dynamic proteins to be fine-tuned, provides new nonmodified Cdc28p targets in each cell cycle, and regulates the degradation of the dynamic proteins through phosphorylation. The latter is supported by an overrepresentation of predicted PEST (regions rich in Pro, Glu, Ser, and Thr) degradation signals among both the dynamic proteins and the putative Cdc28p targets in the network [significant at $P < 10^{-2}$ and $P < 10^{-3}$, respectively (*13*)]. Cell cycle–regulated transcription thus supplies the cell with nonmodified complex components at the time of complex assembly, many of which are later phosphorylated and specifically targeted for degradation.

With the emergence of new large-scale data sets, including assays focused on protein-DNA interactions and transient protein-protein interactions, we expect more of the dynamic proteins to be included in the network. Also, we currently lack information about the life-

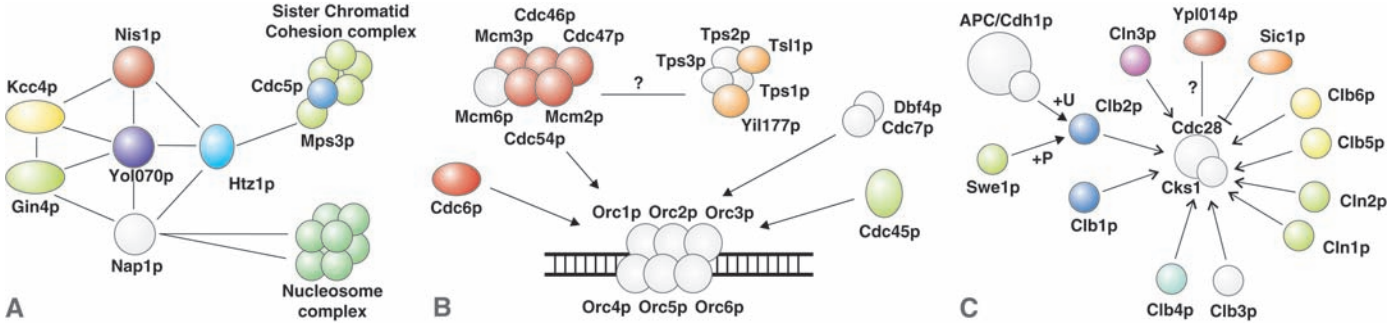

Fig. 3. Dynamic modules. Each panel shows a specific module from the network in Fig. 1, using the corresponding colors of individual proteins. (**A**) Previously unknown module connecting processes related to chromosome structure with mitotic events in the bud. The nucleosome assembly protein Nap1p is known to shuttle between the nucleus and cytosol and regulates the activity of Gin4p, one of two G_1-expressed budding-related kinases in the module. Nap1p and the histone variant Htz1p connect the module to the nucleosome and sister chromatid modules, respectively. Two poorly characterized proteins, Nis1p and the putative Cdc28p substrate Yol070p (*16*), are both expressed in mitosis and localize to the bud neck (*13*). (**B**) Schematic representation of the dynamic assembly of the prereplication complex. It contains six static proteins (Orc1p to Orc6p) that are bound to origins of replication throughout the entire division cycle. A subcomplex of six Mcm proteins is recruited to the ORC complex in G_1 phase by a Cdc6p-dependent mechanism; we see the corresponding genes (except *MCM6*) transcribed just before that. Final recruitment of the replication machinery is dependent on Cdc45p, which we find expressed in early S phase. More details and case stories are available (*13*). (**C**) Cdc28p module, with the different cyclins and interactors placed at their time of synthesis. At the end of mitosis, the cyclins are ubiquitinated and targeted for destruction by APC and SCF, reflected in the network by the interaction between Cdh1p and Clb2p. The latter also interacts with Swe1p, which inhibits entry into mitosis by phosphorylating Cdc28p in complex with Clb-type cyclins. We also discovered an uncharacterized protein, Ypl014p, in this well-studied module (*13*).

time of the observed complexes and modules. With reliable time series of protein abundances, preferably in individual compartments, the resolution of this temporal network can be increased considerably, because even individual interactions over time could then be monitored. Moreover, the integrative approach presented here should be applicable to any biological system for which both interaction data and time series are available.

References and Notes

1. A. L. Barabasi, Z. N. Oltvai, *Nature Rev. Genet.* **5**, 101 (2004).
2. R. J. Cho *et al.*, *Mol. Cell* **2**, 65 (1998).
3. P. T. Spellman *et al.*, *Mol. Biol. Cell* **9**, 3273 (1998).
4. U. de Lichtenberg *et al.*, *Bioinformatics* doi:10.1093/bioinformatics/bti093 (2004).
5. T. Ito *et al.*, *Proc. Natl. Acad. Sci. U.S.A.* **97**, 1143 (2000).
6. P. Uetz *et al.*, *Nature* **403**, 623 (2000).
7. A.-C. Gavin *et al.*, *Nature* **415**, 141 (2002).
8. Y. Ho *et al.*, *Nature* **415**, 180 (2002).
9. H. W. Mewes *et al.*, *Nucleic Acids Res.* **32**, 5539 (2004).
10. A. M. Edwards *et al.*, *Trends Genet.* **18**, 529 (2002).
11. C. von Mering *et al.*, *Nature* **417**, 399 (2002).
12. C. von Mering *et al.*, *Nucleic Acids Res.* **31**, 258 (2003).
13. See supporting information on *Science* Online for details.
14. K. R. Christie *et al.*, *Nucleic Acids Res.* **32**, D311 (2004).
15. L. J. Jensen, P. Bork, *Drug Discovery Today: TARGETS* **3**, 51 (2004).
16. J. A. Ubersax *et al.*, *Nature* **425**, 859 (2003).
17. H. H. McAdams, L. Shapiro, *Science* **301**, 1874 (2003).
18. G. Rustici *et al.*, *Nature Genet.* **36**, 809 (2004).
19. M. L. DePamphilis, *Gene* **310**, 1 (2003).
20. V. Measday, H. McBride, J. Moffat, D. Stillman, B. Andrews, *Mol. Microbiol.* **35**, 825 (2000).
21. I. Simon *et al.*, *Cell* **106**, 697 (2001).
22. T. I. Lee *et al.*, *Science* **298**, 799 (2002).

23. We thank S. Hooper for assistance and M. Knop and members of the Bork group for insightful comments on the manuscript. Supported by grants from the Danish National Research Foundation, the Danish Technical Research Council, Novo Nordisk A/S, and the European Union.

Supporting Online Material

www.sciencemag.org/cgi/content/full/307/5710/724/DC1
Materials and Methods
Fig. S1 to S3
Table S1
References

10 September 2004; accepted 9 December 2004
10.1126/science.1105103

Escape of Intracellular *Shigella* from Autophagy

Michinaga Ogawa,[1] Tamotsu Yoshimori,[3,6] Toshihiko Suzuki,[1,5] Hiroshi Sagara,[2] Noboru Mizushima,[4,5] Chihiro Sasakawa[1,6]*

The degradation of undesirable cellular components or organelles, including invading microbes, by autophagy is crucial for cell survival. Here, *Shigella*, an invasive bacteria, was found to be able to escape autophagy by secreting IcsB by means of the type III secretion system. Mutant bacteria lacking IcsB were trapped by autophagy during multiplication within the host cells. IcsB did not directly inhibit autophagy. Rather, *Shigella* VirG, a protein required for intracellular actin-based motility, induced autophagy by binding to the autophagy protein, Atg5. In nonmutant *Shigella*, this binding is competitively inhibited by IcsB binding to VirG.

During the multiplication of microbes within host cells, bacteria become sequestered in membrane-bound organelles such as phagosomes (*1*–*3*). This event is a key component of host defense against invading microbes. Nevertheless, some invasive bacteria such as *Legionella*, *Salmonella*, *Mycobacteria*, and *Brucella* can block or alter the maturation of the phagosome and can reside in vacuoles (*2*–*7*). Some others such as *Shigella* (*8*, *9*), *Listeria monocytogenes* (*10*), and *Rickettsia conorii* (*11*) can escape from phagosomes into the cytoplasm, multiply, and disseminate into neighboring cells by eliciting actin polymerization. Cytoplasmic pathogens may thus circumvent autophagic events.

IcsB, one of the *Shigella flexneri* effectors, is secreted by means of the type III secretion system (TTSS) of cytoplasmic bacteria and located on the bacterial surface (*12*). The *icsB* mutant is fully invasive and able to escape from the vacuole but is defective in spreading within host cells (*12*).

To clarify the role of IcsB in promoting infection, we investigated the intracellular behaviors of the *icsB* mutant (Δ*icsB*), YSH6000 (wild type; WT), and Δ*icsB*/pIcsB (the *icsB* complement strain). In baby hamster kidney (BHK) cells, although mutants lacking IcsB multiplied as normal for about 3 hours, their growth plateaued 4 hours after invasion (fig. S1A). To characterize intracellular bacteria, we introduced green fluorescent protein plasmid (pGFP) into Δ*icsB* and WT then investigated BHK cells infected with bacteria 4 hours after infection. Δ*icsB*/pGFP colocalized with markers for acidic lysosomes (Lysotracker) or autophagosomes [monodancyl-cadaverin (MDC)], where the bacterial morphology was indistinct. (fig. S1, B and C). WT cells, on the whole, did not colocalize with the same markers: 37.2% of Δ*icsB* bacteria colocalized with lysosomes compared with only 10.2% of WT. Furthermore, when BHK cells expressing GFP-LC3, an autophagosome-specific marker (*13*, *14*), were infected with Δ*icsB* or WT, ~40% of Δ*icsB* was associated with LC3 signal; bacterial shape was also indistinct compared with WT (fig. S1D). To further characterize the Δ*icsB* defect, we exploited MDCK cells (epithelial cells from dog kidney) expressing GFP-LC3 (MDCK/pGFP-LC3 cells), which made it feasible to visualize cytoplasmic organelles and bacteria (Fig. 1A). The number of LC3-positive Δ*icsB* was greater than that of WT throughout the 1 to 6 hours after infection. The LC3-positive population of Δ*icsB* had increased 50% by 6 hours, whereas that of WT remained at 10 to 15% (Fig. 1B). Two hours after infection, WT and Δ*icsB* had similar numbers of actin tails. After 4 hours, however, the population was decreased in Δ*icsB* (fig. S2), presumably because Δ*icsB* was within autophagosomes. The LC3-positive population of the Δ*icsB*/pIcsB was decreased: it fell to a level as low as that of WT (Fig. 1B). Autophagic events can be triggered by amino acid starvation (*13*). MDCK/pGFP-LC3 cells were infected with Δ*icsB* or WT, under amino acid–starved conditions. LC3-positive bacteria in MDCK cells were significantly increased from 10 to 16% (WT) and from 23 to 36% (Δ*icsB*) in response to amino acid deprivation (fig. S3). Conversely, when MDCK cells were treated with known inhibitors of autophagy or of lysosomes, such as Wortmannin, 3-methyladenine (3-MA) or bafilomycin-A1 (Baf-A1), the LC3-positive Δ*icsB* population was markedly decreased (Fig. 1, C and D). In the presence of Baf-A1, fusion of lysosomes with autophagosomes containing Δ*icsB* was blocked, which would have allowed the bacteria to escape into the cytosol. Consistently, despite the smaller diameter (<0.15 mm) of plaques formed by Δ*icsB* 2 days after infection than that of plaques formed by WT (~0.5 mm), the plaque-forming capacity of Δ*icsB* was restored by treatment with Baf-A1 (fig. S4). Another investigation was made in *atg5*-knockout mouse embryonic fibroblasts

[1]Department of Microbiology and Immunology, [2]Department of Fine Morphology, Institute of Medical Science, University of Tokyo, 4-6-1, Shirokanedai, Minato-ku, Tokyo 108-8639, Japan. [3]Department of Cell Genetics, National Institute of Genetics, 1111, Yata, Mishima, Shizuoka 411-8540, Japan. [4]Department of Bioregulation and Metabolism, Tokyo Metropolitan Institute of Medical Science, 3-18-22, Hon-komagome, Bunkyo-ku, Tokyo 113-8613, Japan. [5]Precursory Research for Embryonic Science and Technology (PRESTO), [6]Core Research for Evolutional Science and Technology (CREST), Japan Science and Technology Agency, Kawaguchi 332-0012, Japan.

*To whom correspondence should be addressed. E-mail: sasakawa@ims.u-tokyo.ac.jp